EUV mask surface cleaning effects on lithography process performance

Running title: EUV mask surface cleaning effects on lithography process performance

Running Authors: George, Naulleau, Chen, and Liang

Simi A. George[a)], Lorie Mae Baclea-an and Patrick P. Naulleau

Center for X-ray Optics, Lawrence Berkeley National Laboratory, 1 Cyclotron Road, Berkeley, CA, 94720

Robert J. Chen and Ted Liang

Intel Corporation, Santa Clara, CA 95052

[a)]Electronic Mail: sageorge@lbl.gov

Material Names: Carbon, Ruthenium, Hexamethyldisilazane

The reflective, multilayer based, mask architectures for extreme ultraviolet (EUV) lithography are highly susceptible to surface oxidation and contamination. As a result, EUV masks are expected to undergo cleaning processes in order to maintain the lifetimes necessary for high volume manufacturing. For this study, the impact of repetitive cleaning of EUV masks on imaging performance was evaluated. Two, high quality industry standard, EUV masks are used for this study with one of the masks undergoing repeated cleaning and the other one kept as a reference. Lithographic performance, in terms of process window analysis and line edge roughness, was monitored after every two cleans and compared to the reference mask performance. After 8x clean, minimal degradation is observed. The cleaning cycles will be continued until significant loss imaging fidelity is found.

I. Introduction

Extreme ultraviolet lithography (EUVL) [1-4] mask lifetime[5] is one of the critical challenges to be resolved as the technology is being prepared for high volume manufacturing (HVM). The reflective, multilayer based, mask architectures requisite for EUVL are highly susceptible to surface oxidation and contamination. Contamination of the EUV reticle due to various surface deposition processes leads to the loss of image contrast and exposure latitude in patterning[6, 7]. As a result, achieving workable mask lifetimes necessitate the cleaning of contaminated masks. For this purpose, several mask cleaning methods are being investigated[8,9].

For a mask cleaning process to be practical, negligible negative impact on mask performance after repeated cleaning is a requirement. Mask surface damage and the increased LER that may result from repetitive cleaning still remains a concern. We recently reported lithographic performance comparison of a contaminated mask that was cleaned to a new uncontaminated mask[10]. Our findings indicated that the performance was not significantly affected by the cleaning process while the cleaning process effectively removed significant amount of deposits from the mask pattern sidewalls. Another completed study involved a mask with an outdated architecture, which was imaged before and after cleaning. Lithographic performance analysis showed that the observed resist LER increased significantly after undergoing an intentionally aggressive multiple cleans test.

In this paper, we present data that is compiled from two industry standard EUV masks, with imaging tests performed at multiple intervals of the repetitive use of a single cleaning process. Prior to the start of the cleans, exposure data from two masks with the same architectures were collected using the same resist and exposure conditions. Subsequently, one of the masks is subjected to multiple cleaning cycles and the other one is kept as a reference. The capping layer surface damage at each cleaning interval is examined using atomic force microscopy.

II. Assessing Capping Layer Damage from Cleaning

All previously completed cleaning studies compare a contaminated mask to its performance after cleaning, a contaminated and then cleaned mask performance to another reference mask, or the effects of contamination itself on mask imaging. A systematic evaluation of the effects of cleaning cycles on the capping layer damage and its impact on mask imaging is not reported on to date. For this paper, direct imaging comparison between two new EUV standard masks is completed. Both masks have identical multilayer, capping layer, absorber, and anti-reflection coating architectures. The capping layer used is Ruthenium (Ru) at a 2.5 nm thickness. Any Carbon (C) contamination on the surface of either mask should be minimal, since they have not been in use prior to these set of imaging studies. An industry-developed cleaning process is used repeatedly on one of the masks, while the other mask is kept as it is.

A. Cleaning

Standard wet cleaning chemistries were used to clean the surface of the mask. The process includes three main steps: organic removal by a mixture of sulfuric acid and hydrogen peroxide, DI water rinse and a final particle clean by megasonic spray with SC1 (DI water with diluted ammonium hydroxide and hydrogen peroxide).

B. Surface analysis

In order to monitor damage to the Ru capping layer surface, three dimensional mask surface profiles were obtained using an atomic force microscope (AFM) at periodic intervals of the cleaning. The AFM used for the measurements is a Veeco Dimension 9000 model. This AFM is capable of measuring sub-angstrom level root mean squared (rms) roughness of a surface, with a nominal tip radius of 8nm and a maximum of 12nm[11]. The imaging is completed in tapping mode with minimal damage to the Ru surface. Each AFM image is 256 X 256 pixels, covering an area of 2µm X 2µm giving a lateral resolution of approximately 7.8nm per pixel. Post processing is used to de-convolve the AFM tip radius from the raw data.

C. Mask patterning with the 0.3NA micro-exposure tool

The imaging was performed on the SEMATECH Berkeley MET installed at the Advanced Light Source synchrotron facility at Lawrence Berkeley National Laboratory. Details on the MET can be found elsewhere[12,13, 14]. In the lithographic results presented here, annular illumination was used with an inner sigma of 0.35 and an outer sigma of 0.55.

The resist images were recorded using a top-down SEM and analyzed offline with the software package SuMMIT[15]. More than 1200 images were recorded and analyzed for the studies completed in this paper. For both mask cases, at pristine condition with no previous imaging or cleaning, patterning was completed with a baseline photoresist, BBR-07A. This resist was spin-coated onto a wafer primed with the Hexamethyldisilazane (HMDS) adhesion promoter to

produce a nominal film thickness of 80nm. This resist was also used for lithographic characterization of the cleaned mask after the first two cleans. After the first two cleans, all subsequent imaging was completed using a different baseline EUV resist, BBR-08A, which is shown to have a higher resolution. A film thickness of 60nm on HMDS on wafer is used for this resist. Each data set consisted of an 11 X 11 grid of focus and exposures, called the focus-exposure matrix (FEM). Each focus step was 50nm to give a focal range of approximately 500 nm across the FEM and the exposure doses were varied in 5% exponential steps.

III. Results

A. Surface analysis

The surface topographies recorded with the AFM at fixed intervals of the cleaning cycles were post-processed and analyzed to assess for any detectable capping layer damage . Figure 1 shows the post-processed AFM images of the capping layer surface of the cleaned mask. The first image (left) was obtained before any cleaning was done to the mask and the consecutive images were completed at fixed intervals between cleans. Specifically, images were collected after every two cleans for a total of 8 clean cycles.

The raw-rms roughness values show an increase after 6 cleans, going from 0.09nm to 0.125nm. On the other hand, the mask blanks are qualified at the mid-spatial frequency range (MSFR, 0.1nm – 1.0nm) and these values do not show any notable variations. Same is true for the high spatial frequency range (HSFR), which means that the raw roughness increase is due to an increase in roughness at the low frequencies. We note, however, that the low frequency changes are likely an AFM artifact. All tabulated values for the roughness are given in table 1.

Figure 1: Atomic force microscope scanned and post-processed images of the capping layer surface of the cleaned mask. The first image (left) was obtained before any cleaning was done to the mask and the consecutive images were completed at fixed intervals between cleans. The roughness extracted from the mid-spatial frequency range (0.1nm - 1.0nm) where the mask blanks are qualified does not show variations. We do see that the total roughness(all frequencies) to have increased.

Table 1: Roughness magnitudes extracted from the AFM images of the cleaned mask at set intervals

B. Critical dimension process analysis

Process window data for two sets of vertical, 1:1 line and space patterns were collected for each mask, one set at the critical dimension (CD) of 40 nm and the other at a CD of 36 nm. The mask was cleaned eight times, with imaging completed after the completion of every two cleans. When the cleaned mask was imaged (referred to as the test mask), the reference mask was also imaged enabling us to track system and resist effects over the long time span of this study. This procedure yielded 11 different patterned samples, with an 11 X 11 FEM on each sample, giving 22 different process windows for the two different feature widths evaluated here.

The first comparative analysis that we complete is for the data collected for patterns recorded in the BBR-07A resist. Three cases are compared with this resist; 1) the test mask condition before the start of the cleanings, 2) the reference mask performance, and 3) the test mask condition after it was cleaned two times. All of the process metrics extracted from the

collected images are compiled in table 2, including iso-focal CD, exposure latitude (EL), depth of focus (DOF), and line-edge roughness (LER). The DOF is determined based on an elliptical fit to the +/-10% CD-change process window. For determining the DOF, the ellipse EL is set to have 10% CD variation. The iso-focal feature widths for both sets of patterns are observed to be nearly identical for all conditions, indicating that there is no damage to the mask patterns after two cleans. Both exposure latitude and DOF data for both pattern widths and all cases show less than 5% variation. This is well within the process uncertainty, which is expected to be anywhere from 5 to 10%.

The averaged, 3σ LER can also be found in table 4, where it is seen that the characterized variations in all cases are well below the measurement and calculation uncertainty of ±0.40nm. Figure 2 shows the iso-focal CD matched LER curves for all three cases at 40nm and 36nm CD. Not much variation is seen through focus, when comparing the three curves in both plots. In comparing all these metrics, we can safely assume that having gone through two cleans did not impact mask surface or patterns enough to cause process changes.

Table 2: Process analysis for 1:1 vertical lines and spaces, using BBR-07A resist for 2 cleans

Figure 2: Iso-focal CD matched LER curves for all three cases at, A) 40nm and B) 36nm CD. The averaged, 3σ LER for all cases is near 4.8nm in the best dose and focus region of the process, with the variations shown to be less than the uncertainty computed to be near ±0.4nm.

After two cleans of the test mask, the test resist was changed to BBR-08A. Pattern data for the 40nm and 36nm CD is collected for imaging completed at every two cleans of the test mask and the reference mask on the same day as the test mask imaging. All process data for the two masks at 2 cleans, 4 cleans, 6 cleans and 8 cleans are given in tables 3 and 4. Table 3 shows the comparison between two masks for the 40nm patterns and table 4 gives comparison for 36nm patterns. We note that the process metrics calculated for the reference mask case at the 8 cleans is lower because of a focus shift in the system causing the best/dose focus region of the FEM to be off center creating an incomplete process window. Aside from this, all observed changes in DOF are less than a focus step, which was 50nm for these patterning studies. Figures 3 and 4 shows the compiled EL vs. DOF at the set cleaning intervals of the test mask and the corresponding reference mask data at 40nm and 36nm CDs. In all cases, the absolute change in exposure latitude is less than 5% at the 10% CD variation. This falls within the process stability of the micro-exposure tool patterning, supporting the conclusion that the currently observed differences in the data is not the result of cleaning. We also note that the reference mask shows more variation through process than the cleaned mask, further supporting our conclusions.

The 3σ LER is found to be near 4 nm for all data, and the uncertainty in the image metrology itself is computed to near 0.30nm. Analysis completed on the CD matched patterns from the best dose/focus region shows some increase in LER for the test mask data sets. At the same time, the reference mask data shows greater variation and similar increase in LER. The disparities seen in the two sets of data are not greater than what would be observed from multiple wafer printing with the same mask. Thus, we conclude that the LER differences between the two masks are minimal, supporting the results observed from the CD process window performance.

Table 3: Process comparison of all relevant parameters for 1:1 40nm lines and spaces patterns

Table 4: Process comparison of all relevant parameters for 1:1 36nm lines and spaces patterns

Figure 3: Compiled EL vs. DOF at the set cleaning intervals of the (A) test mask and the corresponding (B) reference mask data for the 40nm equal lines and spaces patterns. The less than 5% changes seen in the exposure latitudes for both mask cases are typical of the wafer to wafer process and systematic errors. The DOF for one of the data sets in the reference mask case is smaller because of a focus error. With this exception, we have all DOFs falling into the same range

Figure 4: Compiled EL vs. DOF at the set cleaning intervals of the (A) test mask and the corresponding (B) reference mask data for the 36nm patterns. All data is similar to the larger pattern widths analyzed.

IV. Summary and Discussion

Many studies have previously shown that mask cleans are detrimental to the Ruthenium capping layer by causing increased LER and decreased process latitude. Identification of cleaning processes that are capable of removing contamination, while preserving the mask surface quality is needed for achieving acceptable EUVL mask lifetimes. For this study, a cleaning method that was found to be effective in removing mask surface contaminants was used to clean an uncontaminated mask surface repeatedly. Systematic evaluation of the surface and imaging performance variations are tracked. AFM based surface analysis results and CD process analysis results are reported here. Thus far, surface analysis data evaluated do not give any cause for concern.

For patterning, two different MET baseline resists were used with annular illumination. Data compiled does not indicate variations beyond what can be expected from wafer to wafer process error. This leads to the obvious conclusion that the cleaning did indeed work, and that the cleaned mask performance is comparable to that of a new mask.

Acknowledgments

We wish to acknowledge the expert support provided by Paul Denham, Gideon Jones, Brian Hoef, and Christopher N. Anderson of the Center for X-Ray Optics at Lawrence Berkeley National Laboratory with the exposure tool as well as the entire CXRO engineering team for building and maintaining the EUV exposure tool. We acknowledge SEMATECH for the support of the SEMATECH Berkeley MET and in particular the programmatic support from Warren Montgomery, Bryan Rice, and Stefan Wurm. This work was supported in part by SEMATECH and carried out at Lawrence Berkeley National Laboratory's Advanced Light Source, which is supported by the DOE, Office of Science and the Basic Energy Sciences under Contract No. DE-AC02-05CH11231.

[1]*EUV Lithography*, edited by V. Bakshi (SPIE Press, Washington, 2007)

[2]B. Wu and A. Kumar, J. Vac. Sci. Technol. B 25, 1743 (2007)

[3]O. Wood, C.-S. Koay, K. Petrillo, H. Mizuno, S. Raghunathan, J. Arnold, D. Horak, M. Burkhardt, G. McIntyre, Y. Deng, B. LaFontaine, U. Okoroanyanwu, A. Tchikoulaeva, T. Wallow, J. H.-C. Chen, M. Colburn, S. S.-C. Fan, B. S. Haran, and Y. Yin, Proc. SPIE **7271,** 727104 (2009)

[4]S. Wurm, F. Goodwin, and H. Yun, Next-generation lithography: *EUVL readiness for pilot line insertion*, Solid State Technology, 52(2), 2009. http://www.solid-state.com/display_article/352195

[5]B. LaFontaine, A. R. Pawloski, Y. Deng, C. Chovino, L. Dieu, O. R. Wood, II, and H. J. Levinson, Proc. SPIE **5374,** 300 (2004)

[6]A Wüest, *EUV Optics/Mask Contamination – Critical Issues Survey Results*, IEUVI Optics Contamination and Lifetime Technical Working Group Presentation, October 2, 2008. http://ieuvi.org/TWG/ConOptics/2008/MTG100208/2-Wuest.pdf

[7]Y-J Fan, L. Yankulin, A. Antohe, P. Thomas, C. Mbanaso, R. Garg, Y. Wang, A. Wuest, F. Goodwin, S. Huh, P. Naulleau, K. Goldberg, I. Mochi, and G. Denbeaux, J. Vac. Sci. Technol. B 28, 321 (2010)

[8]Y. Nishiyama, T. Anazawa, H. Oizumi, I. Nishiyama, O. Suga, K. Abe, S. Kagata, and A. Izumi, Proc. SPIE **6921,** 692116 (2008)

[9]L.Belau, J. Y. Park, T. Liang, H. Seo, and G. A. Somorjai, J. Vac. Sci. Technol. B 27, 1919 (2009).

[10]S.A.George, P. Naulleau; U. Okoroanyanwu; K. Dittmar; C. Holfield; A. Wüest, JVSTB MS# 40551, submitted

[11]K.Miller, and B. Todd, Proc. SPIE, Vol. 4186, pp. 681-687, 2002

[12]P. P. Naulleau, K. A. Goldberg, P. Batson, J. Bokor, P. Denham, and S. Rekawa, Appl. Opt. **42,** 820 (2003)

[13]P. P. Naulleau, C. N. Anderson, J. Chiu, K. Dean, P. Denham, K. A. Goldberg, B. Hoef, S. Huh, G. Jones, B. M. LaFontaine, A. Ma, D. Niakoula, J. Park, and T. Wallow, Proc. SPIE **6921,** 69213N (2008)

[14]P. P. Naulleau, K. A. Goldberg, E. Anderson, J. P. Cain, P. Denham, K. Jackson, A.-S. Morlens, S. Rekawa, and F. Salmassi, J. Vac. Sci. Technol. B **22**, 2962 (2004)

[15]SuMMIT Software Division of EUV Technology, *Summit Litho Image Analysis Software*, 2009. http://www.euvl.com/summit/

List of Tables

Table 1: Extracted rms roughness from AFM surface measurements

	Roughness (nm)			
	Initial	2 cleans	4 cleans	8 cleans
Raw RMS: All frequencies	0.093	0.090	0.125	0.114
Mid-spatial frequency range	0.069	0.069	0.079	0.062
High-spatial frequency range	0.057	0.056	0.060	0.056

Table 2: Process analysis for 1:1 vertical lines and spaces, using BBR-07A resist for 2 cleans

	Iso-focal CD (nm)	Exposure Latitude (%)	DOF (nm)	3σ LER (nm)
40nm 1:1 Lines and spaces				
Reference	39.7	18.7	400.0	4.78 ± 0.45
Test : 0 cleans	40.0	22.3	400.0	4.71 ± 0.39
Test : 2 cleans	39.9	21.1	450.0	4.88 ± 0.43
36nm 1:1 Lines and spaces				
Reference	36.3	19.8	389.5	4.82 ± 0.44
Test : 0 cleans	37.0	22.0	400.0	4.94 ± 0.43
Test : 2 cleans	36.0	21.4	450.0	5.25 ± 0.49

Table 3: Process comparison of all relevant parameters for 1:1 40nm lines and spaces patterns

	Test Mask				Reference Mask			
	Iso-focal CD (nm)	Exposure Latitude	DOF* (nm)	LER_ave (nm)	Iso-focal CD (nm)	Exposure Latitude	DOF* (nm)	LER_ave (nm)
2 cleans	37.25	18.8	400	4.03	39.0	16.6	400	4.21
4 cleans	39.5	16.3	450	3.96	40.0	15.4	450	3.98
6 cleans	39.5	16.0	400	4.24	36.0	13.5	400	4.02
8 cleans	39.5	15.5	450	4.25	36.0	14.7	300**	4.19

*Elliptical Fit, **Missed focus on the reference mask data corresponding to the 8 cleans

Table 4: Process comparison of all relevant parameters for 1:1 36nm lines and spaces patterns

	Test Mask				Reference Mask			
	Iso-focal CD (nm)	Exposure Latitude	DOF* (nm)	LER_ave (nm)	Iso-focal CD (nm)	Exposure Latitude	DOF* (nm)	LER_ave (nm)
2 cleans	34.5	16.5	400	4.13	36.0	16.9	375	4.32
4 cleans	34.0	16.1	400	3.99	36.0	11.9	450	4.14
6 cleans	36.0	14.8	350	4.15	34.25	13.4	350	4.25
8 cleans	35.0	14.0	500	4.01	33.0	12.7	350	4.48

*Elliptical Fit, **Missed focus on the reference mask data corresponding to the 8 cleans

List of Figures

EUV mask surface cleaning effects on lithography process performance

Figure 1: Atomic force microscope scanned and post-processed images of the capping layer surface of the cleaned mask. The first image (left) was obtained before any cleaning was done to the mask and the consecutive images were completed at fixed intervals between cleans. The roughness extracted from the mid-spatial frequency range (0.1nm - 1.0nm) where the mask blanks are qualified does not show variations. We do see that the total roughnesses (all frequencies) have increased.

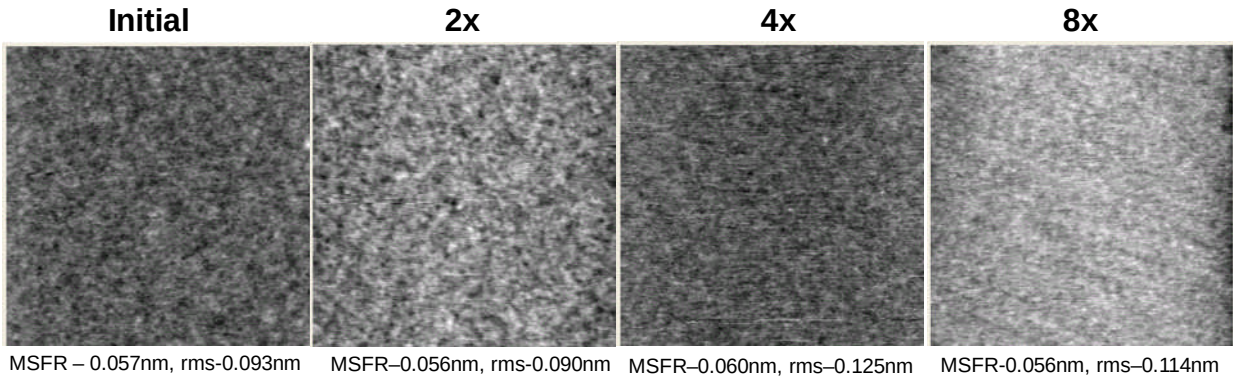

Figure 2: Iso-focal CD matched LER curves for all three cases at, A) 40nm and B) 36nm CD**.** The averaged, 3σ LER for all cases is near 4.8nm in the best dose and focus region of the process, with the variations shown to be less than the uncertainty computed to be near ±0.4nm.

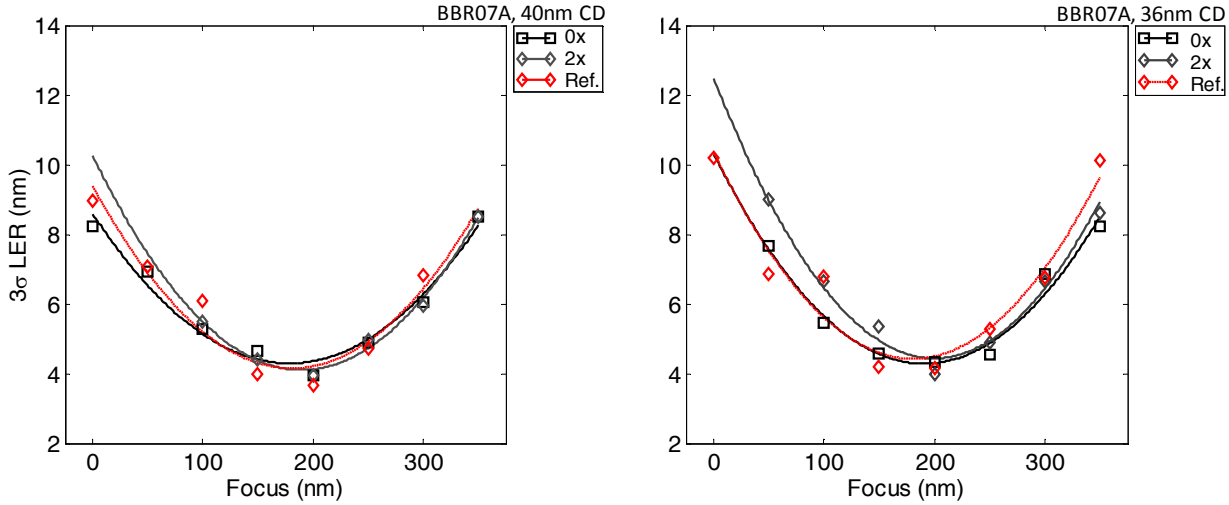

(A) (B)

Figure 3:

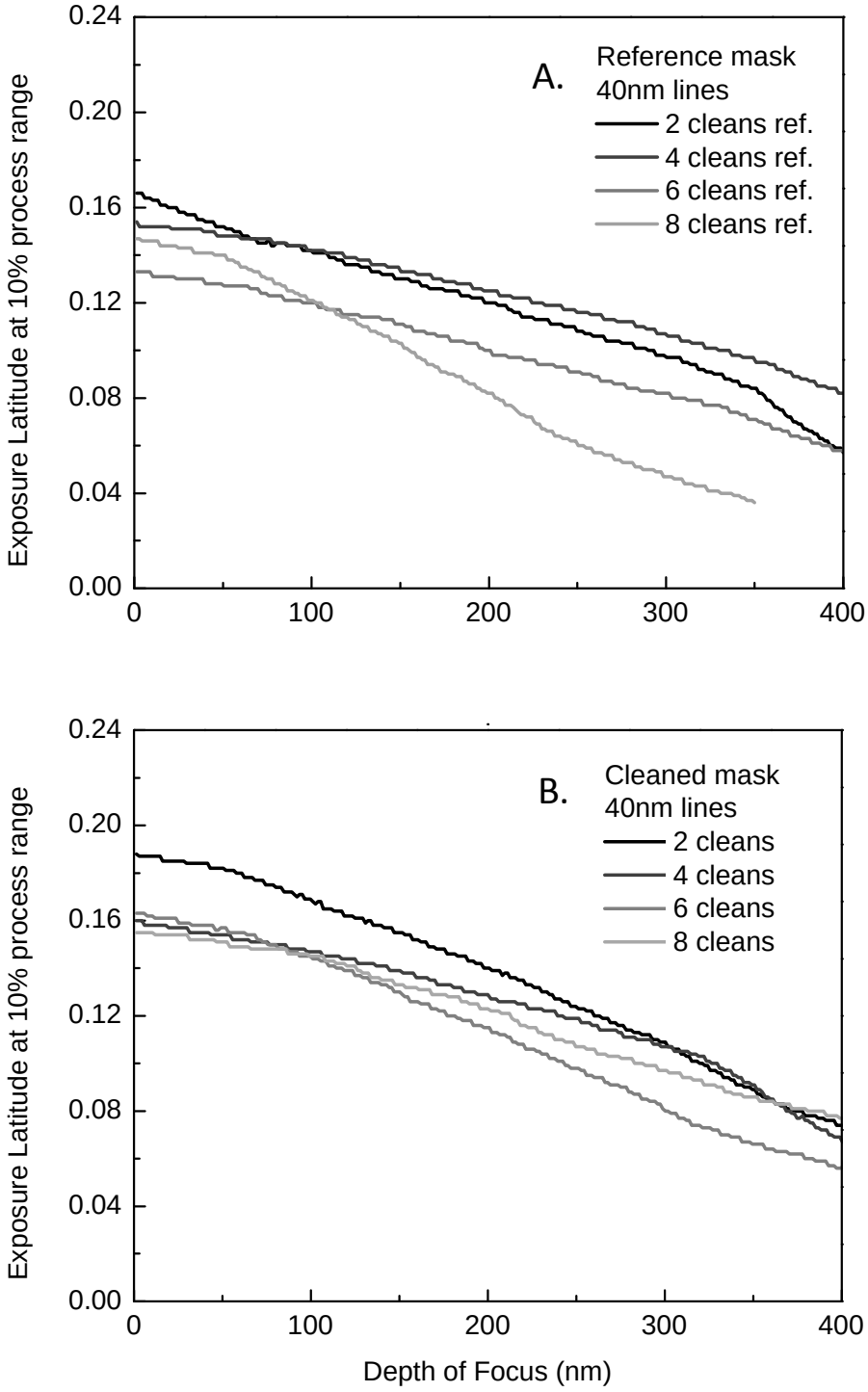
A.
Reference mask
40nm lines
2 cleans ref.
4 cleans ref.
6 cleans ref.
8 cleans ref.
B.
Cleaned mask
40nm lines
2 cleans
4 cleans
6 cleans
8 cleans
Exposure Latitude at 10% process range
Depth of Focus (nm)
0.00
0.04
0.08
0.12
0.16
0.20
0.24
0
100
200
300
400

Figure 4:

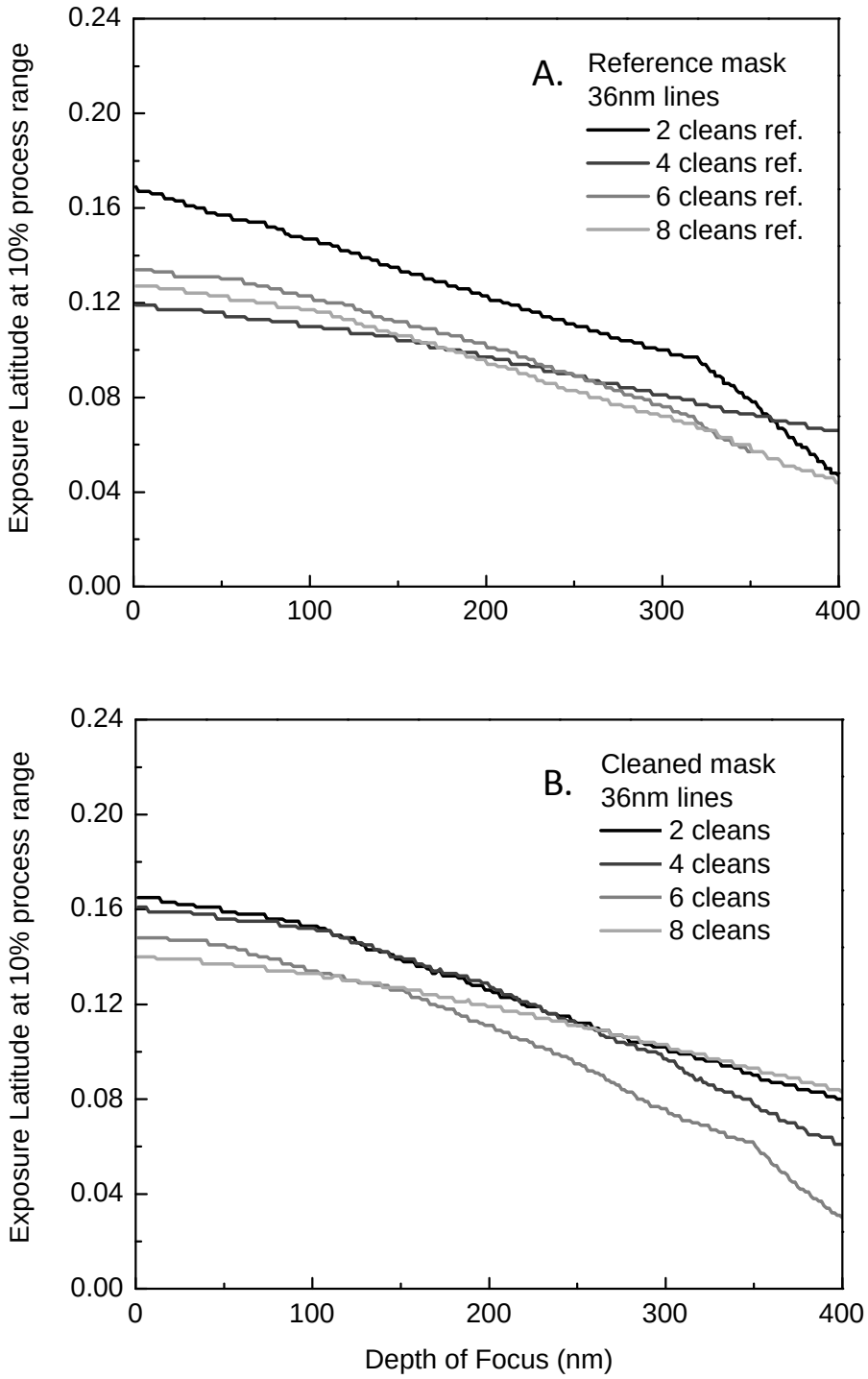
A.
Reference mask
36nm lines
2 cleans ref.
4 cleans ref.
6 cleans ref.
8 cleans ref.
B.
Cleaned mask
36nm lines
2 cleans
4 cleans
6 cleans
8 cleans
Exposure Latitude at 10% process range
Depth of Focus (nm)
0.00
0.04
0.08
0.12
0.16
0.20
0.24
0
100
200
300
400